



**HAL**  
open science

## **Quantitative model of Carbon and Nitrogen isotope composition to highlight sources of nutrient discharge in coastal area (Toulon Bay, NW Mediterranean Sea)**

Duc Huy Dang, R. Douglas Evans, Gaël Durrieu, Amonda El Houssainy, Jean-Ulrich Mullot, N. Layglon, Véronique Lenoble, Stéphane Mounier, Cédric Garnier

### **► To cite this version:**

Duc Huy Dang, R. Douglas Evans, Gaël Durrieu, Amonda El Houssainy, Jean-Ulrich Mullot, et al.. Quantitative model of Carbon and Nitrogen isotope composition to highlight sources of nutrient discharge in coastal area (Toulon Bay, NW Mediterranean Sea). *Chemosphere*, 2018, 194, pp.543 - 552. 10.1016/j.chemosphere.2017.12.109 . hal-01879413

**HAL Id: hal-01879413**

**<https://hal.science/hal-01879413v1>**

Submitted on 29 Sep 2018

**HAL** is a multi-disciplinary open access archive for the deposit and dissemination of scientific research documents, whether they are published or not. The documents may come from teaching and research institutions in France or abroad, or from public or private research centers.

L'archive ouverte pluridisciplinaire **HAL**, est destinée au dépôt et à la diffusion de documents scientifiques de niveau recherche, publiés ou non, émanant des établissements d'enseignement et de recherche français ou étrangers, des laboratoires publics ou privés.

1 **Quantitative model of Carbon and Nitrogen isotope composition to highlight sources of**  
2 **nutrient discharge in coastal sediments (Toulon Bay, NW Mediterranean Sea)**

3  
4 Duc Huy Dang<sup>1,2\*</sup>, R. Douglas Evans<sup>1,3</sup>, Gael Durrieu<sup>2,4</sup>, Nicolas Layglon<sup>2</sup>, Amonda El  
5 Houssainy<sup>2,5</sup>, Jean-Ulrich Mullot<sup>6</sup>, Véronique Lenoble<sup>2,4</sup>, Stéphane Mounier<sup>2,4</sup>, Cédric  
6 Garnier<sup>2,4</sup>

7  
8 <sup>1</sup> School of the Environment, Trent University, 1600 West Bank Drive, Peterborough, ON,  
9 Canada K9L 0G2

10 <sup>2</sup> Université de Toulon, PROTEE, EA 3819, CS60584, 83041 Toulon Cedex 9, France

11 <sup>3</sup> Water Quality Centre, Trent University, 1600 West Bank Drive, Peterborough, ON, Canada  
12 K9L 0G2

13 <sup>4</sup> Université de Toulon, Aix Marseille Université, CNRS, IRD, Mediterranean Institute of  
14 Oceanography (MIO), UMR7294, 83041 Toulon Cedex 9, France

15 <sup>5</sup> Centre National des Sciences Marines, CNRSL, PO Box 534, Batroun, Lebanon

16 <sup>6</sup> LASEM-Toulon, Base Navale De Toulon, BP 61, 83800 Toulon, France

17  
18 \*Corresponding author. Tel: +1 705 748 1011 (ext. 7692).

19 *E-mail:* [huydang@trentu.ca](mailto:huydang@trentu.ca)

20

21 **ABSTRACT**

22 Nutrient loadings from either point or non-point sources to the environments are related to the  
23 growing global population. Subsequent negative impacts of nutrient loading on the  
24 environments requires a better understanding of their biogeochemical cycling and better tools  
25 to track their sources. This study examines the C, N and P discharge and cycling in a  
26 Mediterranean coastal area from rivers to marine sediments and assesses the anthropogenic  
27 contributions. Carbon and N concentrations and isotope compositions in rivers particles,  
28 surface sediments, and sediment cores were investigated to build up a quantitative multiple-  
29 end-member mixing model for C and N isotopes. This model has allowed determining the  
30 contribution of four natural and one anthropogenic sources to the sediments and highlighted  
31 the anthropogenic fraction of P based on the relationship with anthropogenic  $\delta^{15}\text{N}$ . Although  
32 P is a monoisotopic element and P total concentration has been the sole index to study P  
33 loading, this study suggests an alternative approach to differentiate anthropogenic and non-  
34 anthropogenic (diagenetic) P and revealed point and non-point sources of P and the  
35 corresponding P loading. Also, the diagenetic P background has been established for the 50-  
36 cm sediment layer of the whole Bay.

37

38 **KEYWORDS**

39 Isotope composition; Carbon; Nitrogen; Phosphorus; Coastal area; Point and non-point  
40 sources

## 41 1. INTRODUCTION

42 Coastal and estuarine areas are among the most productive, diverse, and economically  
43 important ecosystems for human society, and play a primordial role in C and other nutrients  
44 storage via primary production. However, these ecosystems are widely and globally  
45 threatened, mostly by anthropogenic pressure and impacts of climate change (Hobbie, 2000;  
46 Paerl, 2006; UNEP, 2006; Wetz et al., 2008). One of the greatest threats to these ecosystems  
47 is eutrophication due to nutrients loading by either point (e.g. waste water discharge) or non-  
48 point (e.g. agricultural runoff, atmospheric deposition) sources (Bohlin et al., 2006; Church et  
49 al., 2006; Savage et al., 2010; Vaalgamaa et al., 2013) leading to an increasing frequency of  
50 harmful algal blooms (Kimbrough et al., 2008; Paerl, 2008, 2006; Vitousek et al., 1997).

51 Sedimentary accumulation in organic matter (OM) and C-N isotope composition have been  
52 used widely as a valuable paleo-environmental tool to track origins of the OM and any change  
53 in nutrient availability in surface waters (Bohlin et al., 2006; Church et al., 2006; Di Leonardo  
54 et al., 2012; Harmelin-Vivien et al., 2008; Ogrinc et al., 2005; Teranes and Bernasconi, 2000;  
55 Vaalgamaa et al., 2013; Yokoyama et al., 2006). The carbon source for terrestrial plants is  
56 atmospheric CO<sub>2</sub> with a  $\delta^{13}\text{C}$  which decreased from -7.5‰ in the 1980s to -8.5‰ today,  
57 relative to the Vienna PeeDee Belemnite (Cuntz, 2011). For land vegetation, different  
58 assimilation pathways differentiate C3 and C4 plants by typical  $\delta^{13}\text{C}$  ranges of -24‰ to -34‰  
59 and -10‰ to -20‰, respectively (Dean, 2006; Meyers, 1997). However, most aquatic  
60 vegetation obtains its carbon from dissolved inorganic carbon resulting in  $\delta^{13}\text{C}$  ranging from -  
61 18 to -28 ‰ (Bohlin et al., 2006; Dean, 2006; Kendall et al., 2001). The two latter OM pools  
62 of terrestrial plants (i.e., land and aquatic) are then indistinguishable by  $\delta^{13}\text{C}$ . However, there  
63 is a significant difference in  $\delta^{13}\text{C}$  between terrestrial and marine organic matter (freshwater  
64 and marine phytoplankton: -30 ‰ and 20-22‰, respectively (Bohlin et al., 2006; Bouillon et  
65 al., 2012; Meyers, 1997)). Also, among aquatic marine macrophytes, physiological

66 differences result in variation in  $\delta^{13}\text{C}$  values in seagrasses and macroalgae (Parker, 1964;  
67 Stephenson et al., 1986); a value of  $-10.5\pm 3.3$  ‰ has been reported in 195 observations of  
68 seagrasses (Hemminga and Mateo, 1996) while a range from -12 to -18 ‰ is observed for  
69 macroalgae (Belicka et al., 2012).

70 Concerning N, biogeochemical processes tend to enrich  $^{15}\text{N}$  leading to a positive drift in  $\delta^{15}\text{N}$ ,  
71 except for some methanogenic and nitrogen-fixing organisms (e.g., cyanobacteria) (Cloern et  
72 al., 2002; Dean, 2006). Relative to atmospheric  $\text{N}_2$ ,  $\delta^{15}\text{N}$  ranges from +2‰ to +3‰ in soils  
73 (Vaalgamaa et al., 2013), and -2‰ to +5‰ in chemical fertilizers (Vaalgamaa et al., 2013)  
74 while it ranges between +7‰ to +9‰ in estuarine and marine phytoplankton (Cloern et al.,  
75 2002; Vaalgamaa et al., 2013). Also, a peculiarly high value of  $\delta^{15}\text{N}$  between 10‰ to 25 ‰ is  
76 typical of ammonia volatilization in animal manure (Choi et al., 2003) and could be used to  
77 track agricultural and urban point sources (e.g., treated/untreated sewage discharge) (Bohlin et  
78 al., 2006; Savage et al., 2010; Vaalgamaa et al., 2013). In summary, terrigenous material has  
79 lower values in  $\delta^{15}\text{N}$  and  $\delta^{13}\text{C}$  than estuarine and marine OM (Ogrinc et al., 2005; Vaalgamaa  
80 et al., 2013).

81 Diverse C-N isotope compositions reflect different sources of the OM. Also, early diagenesis  
82 could alter the C-N isotope composition in sediments, mostly by selective degradation of  
83 organic compounds and isotope fractionation during degradation (Ogrinc et al., 2005 and  
84 references therein). However, this alteration is considered less significant for C (i.e., <2‰)  
85 than N (Bohlin et al., 2006; Ogrinc et al., 2005). Nevertheless, contradictory conclusions have  
86 been reported for the direction of N isotopic shift during decomposition. It finally appears that  
87 the observed change in N isotopic composition (if any) is not related to that in the residual N  
88 pool but to the microbially added nitrogen which depends on the N substrate (see discussion  
89 in Bouillon et al. (2012) and Lehmann et al. (2002)). This conclusion supports the hypothesis  
90 that the vertical variation in C and N isotope composition in sediments could be a useful tool

91 to track changes in organic matter input (Church et al., 2006; Teranes and Bernasconi, 2000)  
92 when diagenetic alterations could be negligible (Engel and Macko, 2013; Kohzu et al., 2011).  
93 In addition, eutrophication history could be recorded by C-N isotopes; previous studies  
94 (Church et al., 2006; Teranes and Bernasconi, 2000) have reported (i) a significant positive  
95 correlation between  $\delta^{13}\text{C}$  and total sediment P indicating variations in primary production and  
96 (ii) a change in sedimentary  $\delta^{15}\text{N}$  related to an increase in dissolved nitrate, either by algal  
97 uptake or a variation in N sources (e.g., wastewater vs. agricultural inputs). However, the  
98 diagenetic P cycling is complex; P deposits in sediments in either inorganic or organic forms  
99 which are both releasable in porewater due to carrier phase dissolution (e.g., iron  
100 oxyhydroxides) and organic matter decomposition, potentially followed by P scavenging via  
101 adsorption and/or precipitation processes (Anschutz et al., 2007; Dang et al., 2014a; Krom  
102 and Berner, 1981; Ruttenberg, 2003). Therefore, it is not evident to decipher diagenetic P  
103 enrichment from anthropogenic P in sediments (Anschutz et al., 2007; Dang et al., 2014b;  
104 Ruttenberg, 2003). Unlike C and N, P is a monoisotopic element; it is not possible to track the  
105 P sources and biogeochemical processes controlling P cycling by isotope composition.

106 Globally speaking, the nutrient cycling in coastal areas is challenging due to (i) a multiplicity  
107 of sources (several natural and anthropogenic components), (ii) complex biogeochemical  
108 processes capable of altering original isotope compositions and (iii) reciprocal interactions  
109 with primary production. Resolving this complex system would permit a better evaluation of  
110 the contribution from each source and pinpoint human signatures on nutrient inputs to the  
111 vulnerable coastal areas. However, although multiples OM sources have been identified in  
112 natural coastal sediments, simple mixing models have been used widely with only two end-  
113 members as terrestrial and marine materials (Bohlin et al., 2006; Harmelin-Vivien et al., 2008;  
114 Li et al., 2016; Loneragan et al., 1997; Ogrinc et al., 2005; Ramaswamy et al., 2008). Scarce  
115 are studies on natural sediments with the application of a quantitative multiple-end-member

116 mixing model (Das et al., 2008). However, stable isotope mixing models using multiple  
117 sources have been widely used in food-web studies (see discussion in Erhardt et al. (2014)  
118 and Phillips et al. (2014)). This study aims at developing a quantitative multiple-end-member  
119 mixing model for C and N isotope composition in the coastal sediments of Toulon Bay (NW  
120 Mediterranean Sea) to better highlight anthropogenic contributions to the nutrient balance  
121 (either by point or non-point sources) and sedimentary cycling of these nutrients. The  
122 proposed model is based on C, N, P, Mg and I concentrations and C, N isotope compositions  
123 in several samples of river particles, surface sediments and 50-cm sediment cores at eight  
124 stations of the Bay.

125

## 126 **2. MATERIALS AND METHODS**

### 127 **2.1. Study site and sampling**

128 Samples were collected in Toulon Bay (Fig. 1, NW Mediterranean, SE French coast), hosting  
129 the French Navy Base, yacht clubs, marinas, and aquaculture. Two small urbanized rivers  
130 (Las and Eygoutier) and two treated sewage submarine outlets are the main  
131 terrestrial/anthropogenic inputs to the sea (point sources), in addition to land runoff (non-point  
132 source). The Bay is divided into two non-equal parts, an enclosed western little Bay and a  
133 large Bay open to the sea. Previous studies have revealed serious contamination of the entire  
134 ecosystem of Toulon Bay, and the situation is more dramatic in little Bay than large Bay  
135 (Cossa et al., 2014; Dang et al., 2015a, 2015b, 2014b; Pougnet et al., 2014; Tessier et al.,  
136 2011); in little Bay, the seagrass meadow of *Posidonia oceanica* have totally disappeared for  
137 the last 30 years, harmful phytoplankton has proliferated, and zooplankton diversity was poor  
138 (Bernard et al., 2001; Jamet et al., 2005; Jean et al., 2012).

139 With the support of the French Navy (boats, materials, divers), undisturbed surface and  
140 subsurface sediments (0-5 and 5-10 cm, respectively) were collected from 54 stations situated

141 around the whole Toulon Bay (Fig. 1) using a sediment corer (10-cm diameter and 1-m long  
142 Plexiglas tube) that preserved the sediment-water interface (SWI) (Tessier et al., 2011) in  
143 December 2008, February and June 2009. In addition, sediment cores (~50 cm long) were  
144 collected at eight specific stations (MIS, 3B, LAS1, LAS2, 12, 15, 23 and 52, Fig. 1) during  
145 several sampling campaigns from June 2009 to May 2016 (Dang et al., 2015a). Stations  
146 LAS1, LAS2 and 23 are situated in front of the two main active tributaries of the Bay (Las  
147 and Eygoutier Rivers, Fig. 1) while the former Las river discharged close to station MIS  
148 before it was diverted. Stations MIS, 3B and 12 are located in active military zones with  
149 intense ship traffic, and station 15 is situated in an aquaculture area (fish and mussel farming).  
150 Station 52 is located in large Bay. Sediments were sliced every 2 cm and centrifuged (4000  
151 rpm, 15 min, Sigma 3-18K) within 2 h of collection under inert atmosphere (N<sub>2</sub>). Pore waters  
152 were extracted by filtration of collected supernatants (0.2- m in-line syringe filters, cellulose  
153 nitrate, Sartorius) in an N<sub>2</sub>-purged glove box.

154 In the two tributaries (Las and Eygoutier Rivers), particles traps were deployed by the IRSN  
155 (Radioprotection and Nuclear Safety Institute). Five particle samples were collected in each  
156 tributary during a two-week period from October 2012 to May 2013, mostly during rain  
157 events (Dang et al., 2015b).

158 All solid fractions were frozen (-18°C) in HDPE bottles, freeze-dried, 2-mm sieved and then  
159 kept at -18°C until further treatment.

## 160 **2.2. Sediment analysis**

161 Total Mg, P and Iodine concentrations were determined by X-Ray Fluorescence (Philips PW  
162 2400) equipped with a Rh-tube (detection limit around 0.5%). Particulate organic carbon and  
163 total N were analyzed using either a TOC-V<sub>CSH</sub> analyzer (Shimadzu) or an NCS Flash 2000  
164 analyzer (Thermo Scientific). Analytical details and part of the data have been previously

165 published (Dang et al., 2014a, 2014b; Tessier et al., 2011). Hereafter, C or OC are used for  
166 particulate organic carbon.

167 For C and N stable isotope measurements, sediments were exposed to concentrated HCl vapor  
168 for four days to remove the carbonate matrix. Samples of a few mg were then weighted in tin  
169 capsules and analyzed at the Water Quality Centre (WQC), Trent University, Canada on a  
170 Micromass (Isoprime) Continuous Flow Isotope Ratio Mass Spectrometer (CF-IRMS),  
171 equipped with a Eurovector Elemental Analyzer (EA) for sample introduction. Several blanks  
172 and certified reference materials (i.e., USGS 40 Glutamic Acid Standard, DG(A1) Glutamic  
173 Acid Standard, Casein and High Organic Sediment standard (OAS)) bracketed the samples. A  
174 comparison of the analyzed and certified values is shown in Figure S1. The  $\delta^{13}\text{C}$  and  $\delta^{15}\text{N}$   
175 isotopic ratios are expressed in the usual  $\delta$ -notation (part per mil, ‰), relative to Vienna  
176 PeeDee Belemnite for C and atmospheric  $\text{N}_2$  for N.

### 177 **2.3. Stable isotope mixing model: IsoSource**

178 IsoSource version 1.3.1 (Phillips et al., 2005; Phillips and Gregg, 2003) was used for source  
179 separation, similar to Das et al. (2008). Typically, C and N isotopic composition of several  
180 sources are implemented as inputs of different endmembers. For a sediment sample  
181 (considered as Mixture), the program determines a range of feasible solutions of source  
182 contribution as there are too many combinations to allow a single solution (when the number  
183 of sources is higher than the number of used isotope signatures). For  $n$  sources  $S_i$ , the  
184 observed isotopic signature of the Mixture is the sum of products of individual contribution  
185 ( $f_i$ ) and corresponding signature of the source  $S_i$  ( $\delta^{13}\text{C}_i$ ):

$$\delta^{13}\text{C}_{obs} = \sum_1^n f_i \times \delta^{13}\text{C}_i$$

186 With  $\sum_1^n f_i = 1$ . Same assumption is made for  $\delta^{15}\text{N}$ .

187 Examination of relative contributions of each source was performed with small increments  
188 (1%) and tolerance (0.1). Individual implemented sources in this study will be detailed in  
189 following sections.

190

### 191 **3. RESULTS AND DISCUSSION**

#### 192 **3.1. C, N and P distribution in sediments**

193 The OC and P profiles at station 3B, 12 and 15 were already shown and discussed previously  
194 (Dang et al., 2014b). Averaged concentration in C, N of particles from the two rivers, surface  
195 sediments, and sediment cores at eight stations are summarized in Table 1. Concentrations of  
196 C and P in surface sediments of the whole Bay are shown in Figure 2. Globally, the C and N  
197 profiles are stable all along the core (Dang et al., 2014b) while P profiles, except at station  
198 MIS, are stable from the bottom of the core up to -15 cm then increase to the surface (Figure  
199 S2). This profile has been reported in other coastal environments (Anschutz et al., 2007;  
200 Krom and Berner, 1981) and attributed to either a P loss from sediments to porewater and/or  
201 an upward diffusive flux of P which is scavenged in ferric oxyhydroxide precipitates at the  
202 SWI (Krom and Berner, 1981; Ruttenberg, 2003). Although the C and P concentrations in  
203 surface sediments at the scale of the Bay average ca.  $3.9 \pm 1.5 \%$  and  $530 \pm 150 \text{ g g}^{-1}$  (Table  
204 1), some hot spots in C and P can be noticed: northern parts of little Bay, the aquaculture area  
205 (station 15), and the two outlets of treated sewage (Figure 2) which could suggest there is  
206 non-point (land runoff) and point (aquaculture, sewage outlet) sources in the Bay. However, a  
207 possibility of stronger diagenetic activities at these locations leading to stronger P  
208 accumulation could not be excluded. Also, such surface mapping seems to show a dilution  
209 effect of the Las River particles to the sediment in the north of the Little Bay (Fig. 2); as  
210 particles transported in the Las River consisted of low C, N and P ( $0.9 \%$ ,  $0.07 \%$  and  $410 \text{ g}$

211  $\text{g}^{-1}$ , respectively), lower than that of the Eygoutier River (3 %, 0.21 % and 1240  $\text{g g}^{-1}$ ,  
212 respectively). Although the two watersheds are karstic, Eygoutier River takes its source from  
213 an agricultural area, when the Dardennes dam upstream in the Las should hold back  
214 significantly on particle discharge (Dufresne, 2014; Nicolau et al., 2012). These peculiarities  
215 should explain the difference between the contents of C, N and P in the two rivers.

216 Also, particles from the 2 rivers have similar C/N ratios (*ca.* 14.2  $\text{g g}^{-1}$ ) and surface and  
217 sediment cores presented higher values in C/N ratio (up to 44.9  $\text{g g}^{-1}$ , Fig. 3A). Even when  
218 considering a potential contribution of marine plankton (C/N ratio of 6.6, (Redfield et al.,  
219 1963)), such increase in C/N ratio in sediments compared to sources (terrestrial particles  
220 and/or marine planktons) could be due to the diagenetic preferential degradation of N-rich  
221 compounds (Burdige, 2007; Hammond et al., 1999). In fact, a previous study has shown that  
222 the C/N ratio in porewaters at station 12 was 8.6 ( $\text{g g}^{-1}$ ,  $r^2=0.9$ ,  $n = 275$ ) (Dang et al., 2014a)  
223 when the C/N ratio observed in station-12 sediments was 18.6  $\text{g g}^{-1}$  (Figure 3A). Compared to  
224 the C/N ratio of the river particles of 14.2  $\text{g g}^{-1}$  (Figure 3A), this observation confirms the  
225 diagenetic degradation of N-rich compounds leading to an N-depletion in sediments and N-  
226 enrichment in porewater. Moreover, it seems that the C and N mass balance is preserved  
227 between the residual C and N in sediments and the biologically released C and N in  
228 porewater. This makes the C/N ratio a non-suitable index to track OM source in marine  
229 sediments, except when it is correctly balanced. Similarly for the C and P relationship, the  
230 C/P ratio in river particles is *ca.* 25.7  $\text{g g}^{-1}$  and a P-depletion is observed in sediments (up to  
231 116.7  $\text{g g}^{-1}$  excluding station 15, Fig. 3B).

### 232 3.2. C and N isotope composition

233 Vertical profiles of  $\delta^{13}\text{C}$  and  $\delta^{15}\text{N}$  in river particulate matter and in sediments at eight stations  
234 are summarized in Figure S3. Despite the difference in C and N concentration in particles of

235 the two rivers, C and N isotope compositions are similar with values of  $\delta^{13}\text{C}$  and  $\delta^{15}\text{N}$  of -28.5  
236 ‰ and 5.0 ‰, respectively (Table 1). The  $\delta^{13}\text{C}$  profiles in sediment cores were uniformly  
237 stable; the standard deviation being less than 10‰ of the average value (Figure S3 A, B, Table  
238 1). The  $\delta^{13}\text{C}$  average ranges from -30.1 to -15.8 ‰ with the most negative values observed at  
239 stations MIS, LAS1 and LAS2, probably due to the impact of the delivered particles. In these  
240 three sediment cores,  $\delta^{15}\text{N}$  profiles were among the most stable while other sediments cores  
241 showed a clear  $^{15}\text{N}$  depletion profile from the top to the bottom of the core (Figure S3 C, D).  
242 By gathering paired values of  $\delta^{13}\text{C}$  and  $\delta^{15}\text{N}$  from the literature on C and N isotope  
243 composition in coastal areas (Table S1 and Figure S4), three main zones including freshwater  
244 phytoplankton, estuarine-marine phytoplankton and macroalgae/seagrasses (Figure S4) cover  
245 most of the  $\delta^{13}\text{C}$ - $\delta^{15}\text{N}$  biplot in the Toulon Bay sediments (Figure 4). However, within the C  
246 and N isotope signature of macroalgae/seagrasses, several studies have shown that some  
247 macroalgae were more depleted in  $^{13}\text{C}$  than seagrasses, probably due to the physiological  
248 morphology and the C uptake mechanisms (Alomar et al., 2016; Hemminga and Mateo, 1996;  
249 Jennings et al., 1997; Stephenson et al., 1986). Therefore, while compared to the data in the  
250 Toulon Bay, we have divided the macroalgae/seagrasses group into an additional fourth group  
251 containing solely  $^{13}\text{C}$ - and  $^{15}\text{N}$ -depleted values reported for macroalgae (Table S1, Figure S4).  
252 Consequently, four natural sources are compiled from the literature (i) S1: freshwater  
253 phytoplankton, (ii) S2: estuarine-marine phytoplankton, (iii) S3: seagrasses/macroalgae and  
254 (iv) S4: macroalgae. In addition, one anthropogenic source (Source A) could be implemented.  
255 For that, at stations MIS, 3B, 12, 15 and 23, a significant correlation between  $\delta^{13}\text{C}$  and P is  
256 observed ( $n = 28$ ,  $r^2 = 0.71$ ,  $p < 0.0001$ ) reveals that such high accumulation in P (up to 1400  
257  $\text{g g}^{-1}$  at station MIS) could be an anthropogenic input in the area, together with a specific  
258 signature of C. The corresponding  $\delta^{13}\text{C}$  of the source A was then assumed to that of the

259 sample the most concentrated in P ( $\delta^{13}\text{C}_{\text{sourceA}} = -26.5 \text{ ‰}$ ). The  $\delta^{15}\text{N}_{\text{sourceA}}$  was assumed to be  
260 10 ‰, as usually found for anthropogenic N isotope composition from urban and aquaculture  
261 impacts (Savage et al., 2010; Yokoyama et al., 2006). These five sources (Figure 4) have been  
262 utilized in the IsoSource program to calculate the respective contribution of each individual  
263 source to the observed C and N isotope composition in Toulon Bay sediments.

### 264 **3.3. A quantitative multiple-endmember mixing model for C and N isotope composition**

265 Outputs of the IsoSource model are relative contributions of each of five sources previously  
266 defined. The modeled C and N isotope composition is compared to that observed in sediments  
267 (Figure 5). For C, the model has calculated well the isotope composition of all sediments  
268 (Figure 5A). However, the model has predicted well for only 80 percent of the dataset of N  
269 and there is an offset of 1.15 ‰ concerning 20 ‰ of the samples having the largest  
270 contributions of Source 4 (Figure 5B). This includes the samples the most depleted in  $^{15}\text{N}$ .  
271 The offset of 1.15 ‰ falls within the error of the source 4 ( $\delta^{15}\text{N}_{\text{Source4}} = 1.5 \pm 1.2 \text{ ‰}$ ) and the  
272 difference between the average (1.5 ‰) and the most depleted value recorded in our sediments  
273 (Figure 4). Other studies have already reported *Caulerpa sp.*, the most important invasive  
274 macroalgae in the Mediterranean Sea (Alomar et al., 2016), with such depletion in  $^{15}\text{N}$  ( $\delta^{15}\text{N}$   
275 =  $0.3 \pm 0.43 \text{ ‰}$  to  $1.7 \pm 0.56 \text{ ‰}$ ) and a similar composition in C ( $\delta^{13}\text{C} = -23 \pm 0.51 \text{ ‰}$  to -  
276  $20.1 \pm 0.26 \text{ ‰}$ ) to our sediments (Loneragan et al., 1997). However, without a confirmation of  
277 the isotopic composition of macroalgae populations in Toulon Bay, the averaged isotope  
278 composition of Source4 is not shifted assuming that the model for N isotope is still considered  
279 correct (slope = 1.03,  $r^2 = 0.79$ , Figure 5B) and taking into account analytical and modeling  
280 errors. Also, this model did not take into account stations LAS1 and LAS2 as their C and N  
281 isotopic composition did not fall in the zone defined by the five sources. That would require  
282 an additional source depleted in both  $^{13}\text{C}$  and  $^{15}\text{N}$  (Figure 4). Such situation has been reported

283 for a coastal wetland ( $\delta^{15}\text{N} = 0.7 \pm 0.8 \text{ ‰}$  and  $\delta^{13}\text{C} = -26.8 \pm 1 \text{ ‰}$  (Li et al., 2016)). Nevertheless,  
284 without having investigated in the signature of the Toulon Bay “urban” wetland, this fifth  
285 natural source is not added in the model.

286 Contributions of each of the five sources to the C and N isotope composition in six sediments  
287 cores are summarized in radar plots (Figure 6). For station MIS, sources 1 and 4 are dominant  
288 while at the station 3B, C and N isotope compositions are predicted to be from all five sources  
289 with a slightly higher contribution from source 2. Stations 12 and 15 are similar, with a strong  
290 contribution of source 3. From land to sea, the contribution of Source 4 increases from land to  
291 sea to reach equal contribution with Source 3 at station 23, and dominant contribution at  
292 station 52. In summary, there is a transition of the relative source contributions from the coast  
293 to the open part of the Bay (i.e., from station MIS to 52). Station MIS which is the most  
294 northern in little Bay is strongly influenced by the terrestrial input (Source 1). Station 3B  
295 which is situated in a zone where macrophytes are devastated has equal contributions from all  
296 sources with a slight dominance of marine phytoplankton signature (Source 2). Stations 12  
297 and 15 are located in a shallow water-column zone and have a strong seagrass signature  
298 (Source 3). In the large Bay, C and N isotope compositions seemed to be depleted in  $^{15}\text{N}$   
299 which can result from the presence of macroalgae (Source 4). However, as concentrations in  
300 C and N at these stations are lower than other stations, the influence of diagenetic alteration  
301 on C and N isotope composition could be more significant than for the rest of the Bay.

302  
303 As the anthropogenic contribution could be from either non-point (runoff) or point (treated  
304 sewage) sources, contributions of Source 1 (terrestrial input) and Source A (Anthropogenic  
305 source) were used to evaluate the anthropogenic signature of N isotope composition  
306 ( $\delta^{15}\text{N}_{\text{anthr.}}$ ):

$$\delta^{15}N_{anthr.} = f_{source1} \times \delta^{15}N_{source1} + f_{sourceA} \times \delta^{15}N_{sourceA}$$

307 For stations where these sources are recurrent, this calculation revealed a significant  
308 relationship between total P and  $\delta^{15}N_{anthr.}$  rather than  $\delta^{15}N_{bulk}$  (Figure 7); this P- $\delta^{15}N_{anthr.}$   
309 relationship involves stations MIS, 3B and 12, demonstrating a potential co-contamination of  
310 P and anthropogenic N in the northern part of the Bay. On the other hand, when comparing  
311 total P to total I and Mg in sediments of the whole system (Figure 8), strong relationships are  
312 observed among them, only at stations 15, 23 and 52 but not for those where P is correlated to  
313  $\delta^{15}N_{anthr.}$  (i.e., MIS, 3B and 12). In fact, Iodine is released in sediment porewater as an organic  
314 matter decomposition product in anoxic conditions, then converted into solid phases in oxic  
315 conditions due to the affinity to iron oxyhydroxide (Gao et al., 2003; Ullman and Aller, 1980;  
316 Xianhao et al., 1992). Similar diagenetic behavior is stated for P (Ruttenberg, 2003). In  
317 addition, there is a negative correlation between Mg and P at stations 15, 23 and 52 (Figure  
318 8B), which confirms once again that P accumulation in these stations is related to diagenetic  
319 processes as Mg is accumulated by carbonate mineral precipitation where  $CO_2$  is released  
320 from organic carbon oxidation (Metzger et al., 2007). The correlation between Iodine, Mg and  
321 P in sediments at station 15, 23 and 52 (Figure 8) supports the hypothesis that diagenetic  
322 reactions are the major processes leading to P accumulation at these stations but not an  
323 additional anthropogenic input. These approaches (as shown in Figures 7 and 8) allow us to  
324 differentiate the anthropogenic and “non-anthropogenic/diagenetic” pools of P in coastal  
325 sediments.

326 Eventually, applying the multiple end-member mixing model for C and N and the relationship  
327 to P for the surface sediments of the whole Toulon Bay ( $P_{anthr.} = 270 \times \delta^{15}N_{anthr.}$ , Figure 7),  
328 surface (0-5 cm) distribution of anthropogenic P was calculated (Figure 9). This revealed a  
329 non-point source with strong P loading in the northern part of the little Bay and several point

330 sources at stations 15 (aquaculture area), 39 and 42 (treated sewage outlet). This supports not  
331 only the validity of the model but also the applicability of the approach to detecting  
332 anthropogenic P loading in coastal sediments. This approach seems to be more refined than  
333 using total OC and/or P as shown in Figure 2.

334 In addition, the non-anthropogenic P is calculated as the difference between total P and  $P_{\text{anthr}}$ .  
335 in six sediments cores (Figure 10). The applied model allowed us to assess the background of  
336 P in the Bay and revealed P accumulation only by diagenetic reactions just below the SWI.  
337 Indeed, from various profiles of total P in several sediments cores within the Bay (range of  
338 300-2000  $\text{g g}^{-1}$ , Figure S2), the non-anthropogenic P profiles for six stations were identical  
339 (Figure 10A) with a typical stable background P concentration of  $350 \pm 60$  (2sd)  $\text{g g}^{-1}$  and an  
340 diagenetic accumulation leading up to 60 % of the P background concentration at the top  
341 sediment layer (Figure 10B).

342

#### 343 **4. CONCLUSIONS**

344 C and N isotope ratios have been proven to be useful proxies to (i) decode biogeochemical  
345 processes involving the organic matter, (ii) to study the food web and (iii) to assess ecological  
346 impacts in a changing world. However, relatively few studies exist that have developed  
347 quantitative mixing models for C and N isotopes with multiple sources taken into account.

348 This study has shown:

349 - The applicability of such quantitative multiple end-member mixing models for C and N  
350 isotopes to track organic matter and nutrient sources in coastal environments.

351 - The possibility to differentiate anthropogenic N and P from diagenetic accumulation (“non-  
352 anthropogenic”).

353 - An estimate of point and non-point sources of P in the coastal area of Toulon Bay (runoff  
354 and aquaculture-treated sewage, respectively).

355 - An evaluation of the sedimentary P background profile for the whole Bay of Toulon.

### 356 **ACKNOWLEDGEMENTS:**

357 This study was part of the MerMex-MERITE/MISTRALS research program (part of the  
358 international IMBER, LOICZ, and SOLAS projects), and funded through the CARTOCHIM,  
359 CARTOC, PREVENT and METFLUX research programs (funded by "Toulon-Provence-  
360 Méditerranée (TPM)", the "Région PACA", the "Conseil Départemental du Var" and  
361 "l'Agence de l'Eau Rhône-Méditerranée et Corse"). DHD's Ph.D. and postdoctoral  
362 fellowships were respectively supported by the French Ministry of National Education,  
363 Higher Education and Research and a Canadian NSERC (Natural Sciences and Engineering  
364 Research Council) Collaborative Research and Development Grant to RDE, which also  
365 funded the analyses carried out at the Trent WQC. The authors wish to thank the French Navy  
366 for diving and sampling assistance, Dr. Jean-Francois Koprivnjak for isotope measurements.

367

### 368 **REFERENCES**

369 Alomar, C., Deudero, S., Andaloro, F., Castriota, L., Consoli, P., Falautano, M., Sinopoli, M.,  
370 2016. *Caulerpa cylindracea* Sonder invasion modifies trophic niche in infralittoral rocky  
371 benthic community. *Mar. Environ. Res.* 120, 86–92.  
372 doi:10.1016/j.marenvres.2016.07.010

373 Anschutz, P., Chaillou, G., Lecroart, P., 2007. Phosphorus diagenesis in sediment of the Thau  
374 Lagoon. *Estuar. Coast. Shelf Sci.* 72, 447–456. doi:10.1016/j.ecss.2006.11.012

375 Belicka, L.L., Burkholder, D., Fourqurean, J.W., Heithaus, M.R., MacKo, S.A., Jaffé, R., 2012.  
376 Stable isotope and fatty acid biomarkers of seagrass, epiphytic, and algal organic matter  
377 to consumers in a pristine seagrass ecosystem. *Mar. Freshw. Res.* 63, 1085–1097.  
378 doi:10.1071/MF12027

- 379 Bernard, G., Denis, J., Deneux, F., Belsher, T., Sauzade, D., Boudouresque, C.F., Charbonnel,  
380 E., Emery, E., Herve, G., Bonhomme, P., 2001. Etude et cartographie des biocénoses de  
381 la rade de Toulon, in: Contrat D'étude Pour Le Syndicat Intercommunal de l'Aire  
382 Toulonnaise, Ifremer et GISPosidonie. Ifremer Publ, La Seyne, p. 150.
- 383 Bohlin, H.S., Mörth, C.M., Holm, N.G., 2006. Point source influences on the carbon and  
384 nitrogen geochemistry of sediments in the Stockholm inner archipelago, Sweden. *Sci.*  
385 *Total Environ.* 366, 337–349. doi:10.1016/j.scitotenv.2005.07.016
- 386 Bouillon, S., Connolly, R.M., Gillikin, D.P., 2012. Use of Stable Isotopes to Understand Food  
387 Webs and Ecosystem Functioning in Estuaries, *Treatise on Estuarine and Coastal*  
388 *Science*. Elsevier Inc. doi:10.1016/B978-0-12-374711-2.00711-7
- 389 Burdige, D.J., 2007. Preservation of organic matter in marine sediments: controls,  
390 mechanisms, and an imbalance in sediment organic carbon budgets? *Chem. Rev.* 107,  
391 467–85. doi:10.1021/cr050347q
- 392 Choi, W.J., Lee, S.M., Ro, H.M., 2003. Evaluation of contamination sources of groundwater  
393 NO<sub>3</sub>– using nitrogen isotope data: A review. *Geosci. J.* 7, 81–87.
- 394 Church, T.M., Sommerfield, C.K., Velinsky, D.J., Point, D., Benoit, C., Amouroux, D., Plaa,  
395 D., Donard, O.F.X., 2006. Marsh sediments as records of sedimentation, eutrophication  
396 and metal pollution in the urban Delaware Estuary. *Mar. Chem.* 102, 72–95.  
397 doi:10.1016/j.marchem.2005.10.026
- 398 Cloern, J., Canuel, E., Harris, D., 2002. Stable carbon and nitrogen isotope composition of  
399 aquatic and terrestrial plants of the San Francisco Bay estuarine system. *Limnol.*  
400 *Oceanogr.* 47, 713–729.
- 401 Cossa, D., Garnier, C., Buscail, R., Elbaz-Poulichet, F., Mikac, N., Patel-Sorrentino, N.,  
402 Tessier, E., Rigaud, S., Lenoble, V., Gobeil, C., 2014. A Michaelis–Menten type  
403 equation for describing methylmercury dependence on inorganic mercury in aquatic  
404 sediments. *Biogeochemistry* 119, 35–43. doi:10.1007/s10533-013-9924-3
- 405 Cuntz, M., 2011. Carbon cycle: A dent in carbon's gold standard. *Nature* 477, 547–548.  
406 doi:10.1038/477547a
- 407 Dang, D.H., Lenoble, V., Durrieu, G., Mullot, J.-U., Mounier, S., Garnier, C., 2014a.

408 Sedimentary dynamics of coastal organic matter: An assessment of the porewater  
409 size/reactivity model by spectroscopic techniques. *Estuar. Coast. Shelf Sci.* 151, 100–  
410 111. doi:10.1016/j.ecss.2014.10.002

411 Dang, D.H., Lenoble, V., Durrieu, G., Omanović, D., Mulot, J.-U., Mounier, S., Garnier, C.,  
412 2015a. Seasonal variations of coastal sedimentary trace metals cycling: Insight on the  
413 effect of manganese and iron (oxy)hydroxides, sulphide and organic matter. *Mar. Pollut.*  
414 *Bull.* 92, 113–124. doi:10.1016/j.marpolbul.2014.12.048

415 Dang, D.H., Schaefer, J., Brach-Papa, C., Lenoble, V., Durrieu, G., Dutruch, L., Chiffoleau,  
416 J.-F., Gonzalez, J.-L., Blanc, G., Mulot, J.U., Mounier, S., Garnier, C., 2015b.  
417 Evidencing the impact of coastal contaminated sediments on mussels through Pb stable  
418 isotopes composition. *Environ. Sci. Technol.* 49, 11438–11448.  
419 doi:10.1021/acs.est.5b01893

420 Dang, D.H., Tessier, E., Lenoble, V., Durrieu, G., Omanović, D., Mulot, J.-U., Pfeifer, H.-R.,  
421 Mounier, S., Garnier, C., 2014b. Key parameters controlling arsenic dynamics in coastal  
422 sediments: an analytical and modeling approach. *Mar. Chem.* 161, 34–46.

423 Das, B., Nordin, R., Mazumder, A., 2008. An alternative approach to reconstructing organic  
424 matter accumulation with contrasting watershed disturbance histories from lake  
425 sediments. *Environ. Pollut.* 155, 117–124. doi:10.1016/j.envpol.2007.10.031

426 Dean, W.E., 2006. Characterization of Organic Matter in Lake Sediments from Minnesota and  
427 Yellowstone National Park, U.S. Geological Survey Open-File Report 2006-1053.

428 Di Leonardo, R., Cundy, A.B., Bellanca, A., Mazzola, A., Vizzini, S., 2012. Biogeochemical  
429 evaluation of historical sediment contamination in the Gulf of Palermo (NW Sicily):  
430 Analysis of pseudo-trace elements and stable isotope signals. *J. Mar. Syst.* 94, 185–196.  
431 doi:10.1016/j.jmarsys.2011.11.022

432 Dufresne, C., 2014. Compréhension et analyse des processus hydrosédimentaires dans la baie  
433 de Toulon. Apport à la modélisation de la dispersion des radionucléides. Université de  
434 Toulon.

435 Engel, M., Macko, S.A., 2013. *Organic Geochemistry: Principles and Applications*. Springer  
436 Science & Business Media.

- 437 Erhardt, E.B., Wolf, B.O., Ben-David, M., Bedrick, E.J., 2014. Stable Isotope Sourcing Using  
438 Sampling. *Open J. Ecol.* 4, 289–298. doi:10.4236/oje.2014.46027
- 439 Gao, A.G., Liu, Y.G., Zhang, D.J., Sun, H.Q., 2003. Latitudinal distribution of iodine in  
440 sediments in the Chukchi Sea and the Bering Sea. *Sci. China Ser. D-Earth Sci.* 46, 592–  
441 602. doi:10.1360/03yd9052
- 442 Hammond, D.E., Giordani, P., Berelson, W.M., Poletti, R., 1999. Diagenesis of carbon and  
443 nutrients and benthic exchange in sediments of the Northern Adriatic Sea. *Mar. Chem.*  
444 53–79.
- 445 Harmelin-Vivien, M., Loizeau, V., Mellon, C., Beker, B., Arlhac, D., Bodiguel, X., Ferraton,  
446 F., Hermand, R., Philippon, X., Salen-Picard, C., 2008. Comparison of C and N stable  
447 isotope ratios between surface particulate organic matter and microphytoplankton in the  
448 Gulf of Lions (NW Mediterranean). *Cont. Shelf Res.* 28, 1911–1919.  
449 doi:10.1016/j.csr.2008.03.002
- 450 Hemminga, M.A., Mateo, M.A., 1996. Stable carbon isotopes in seagrasses: Variability in  
451 ratios and use in ecological studies. *Mar. Ecol. Prog. Ser.* 140, 285–298.  
452 doi:10.3354/meps140285
- 453 Hobbie, J.E., 2000. *Estuarine Science: A Synthetic Approach to Research and Practice.*  
454 Washington, DC.
- 455 Jamet, J.L., Jean, N., Bogé, G., Richard, S., Jamet, D., 2005. Plankton succession and  
456 assemblage structure in two neighbouring littoral ecosystems in the north-west  
457 Mediterranean Sea. *Mar. Freshw. Res.* 56, 69–83. doi:10.1071/MF04102
- 458 Jean, N., Dumont, E., Durrieu, G., Balliau, T., Jamet, J.-L., Personnic, S., Garnier, C., 2012.  
459 Protein expression from zooplankton communities in a metal contaminated NW  
460 mediterranean coastal ecosystem. *Mar. Environ. Res.* 80, 12–26.  
461 doi:10.1016/j.marenvres.2012.06.004
- 462 Jennings, S., Reñones, O., Morales-Nin, B., Polunin, N.V.C., Moranta, J., Coll, J., 1997.  
463 Spatial variation in the  $^{15}\text{N}$  and  $^{13}\text{C}$  stable isotope composition of plants, invertebrates  
464 and fishes on Mediterranean reefs: Implications for the study of trophic pathways. *Mar.*  
465 *Ecol. Prog. Ser.* 146, 109–116. doi:10.3354/meps146109

- 466 Kendall, C., Silva, S.R., Kelly, V.J., 2001. Carbon and nitrogen isotopic compositions of  
467 particulate organic matter in four large river systems across the United States. *Hydrol.*  
468 *Process.* 15, 1301–1346. doi:10.1002/hyp.216
- 469 Kimbrough, K.L., Johnson, W.E., Lauenstein, G.G., Chrstensen, J.D., Apeti, D.A., 2008. An  
470 assessment of two decades of contaminant monitoring in the nation's coastal zone. Silver  
471 Spring, MD. NOAA Technical Memorandum NOS NCCOS 74. Silver Spring, MD.
- 472 Kohzu, A., Imai, A., Ohkouchi, N., Fukushima, T., Kamiya, K., Komatsu, K., Tomioka, N.,  
473 Kawasaki, N., Miura, S., Satou, T., 2011. Direct evidence for the alteration of  $^{13}\text{C}$   
474 natural abundances during early diagenesis in Lake Kasumigaura, Japan. *Geochemistry,*  
475 *Geophys. Geosystems* 12, 1–14. doi:10.1029/2011GC003532
- 476 Krom, M.D., Berner, R.A., 1981. The diagenesis of phosphorus in a nearshore marine  
477 sediment. *Geochim. Cosmochim. Acta* 45, 207–216. doi:10.1016/0016-7037(81)90164-2
- 478 Lehmann, M., Bernasconi, S., Barbieri, A., McKenzie, J., 2002. Preservation of organic  
479 matter and alteration of its carbon and nitrogen isotope composition during simulated  
480 and in situ early sedimentary diagenesis. *Geochim. Cosmochim. Acta* 66, 3573–3584.  
481 doi:10.1016/S0016-7037(02)00968-7
- 482 Li, Y., Zhang, H., Tu, C., Fu, C., Xue, Y., Luo, Y., 2016. Sources and fate of organic carbon  
483 and nitrogen from land to ocean: Identified by coupling stable isotopes with C/N ratio.  
484 *Estuar. Coast. Shelf Sci.* 181, 114–122. doi:10.1016/j.ecss.2016.08.024
- 485 Loneragan, N.R., Bunn, S.E., Kellaway, D.M., 1997. Are mangroves and seagrasses sources  
486 of organic carbon for penaeid prawns in a tropical Australian estuary? A multiple stable-  
487 isotope study. *Mar. Biol.* 130, 289–300. doi:10.1007/s002270050248
- 488 Metzger, E., Simonucci, C., Viollier, E., Sarazin, G., Prévot, F., Jézéquel, D., 2007. Benthic  
489 response to shellfish farming in Thau lagoon: Pore water signature. *Estuar. Coast. Shelf*  
490 *Sci.* 72, 406–419. doi:10.1016/j.ecss.2006.11.011
- 491 Meyers, P.A., 1997. Organic geochemical proxies of paleoceanographic, plaeolimnologic, and  
492 plaeoclimatic processes. *Org. Geochem.* 27, 213–250.
- 493 Nicolau, R., Lucas, Y., Merdy, P., Raynaud, M., 2012. Base flow and stormwater net fluxes  
494 of carbon and trace metals to the Mediterranean sea by an urbanized small river. *Water*

495 Res. 46, 6625–6637. doi:10.1016/j.watres.2012.01.031

496 Ogrinc, N., Fontolan, G., Faganeli, J., Covelli, S., 2005. Carbon and nitrogen isotope  
497 compositions of organic matter in coastal marine sediments (the Gulf of Trieste, N  
498 Adriatic Sea): Indicators of sources and preservation. *Mar. Chem.* 95, 163–181.  
499 doi:10.1016/j.marchem.2004.09.003

500 Paerl, H., 2008. Nutrient and other environmental controls of harmful cyanobacterial blooms  
501 along the freshwater-marine continuum. *Adv. Exp. Med. Biol.* 619, 217–37.  
502 doi:10.1007/978-0-387-75865-7\_10

503 Paerl, H.W., 2006. Assessing and managing nutrient-enhanced eutrophication in estuarine and  
504 coastal waters: Interactive effects of human and climatic perturbations. *Ecol. Eng.* 26,  
505 40–54. doi:10.1016/j.ecoleng.2005.09.006

506 Parker, P., 1964. The biogeochemistry of the stable isotopes of carbon in a marine bay.  
507 *Geochim. Cosmochim. Acta* 28, 1155–1164. doi:10.1016/0016-7037(64)90067-5

508 Phillips, D.L., Gregg, J.W., 2003. Source partitioning using stable isotopes: Coping with too  
509 many sources. *Oecologia* 136, 261–269. doi:10.1007/s00442-003-1218-3

510 Phillips, D.L., Inger, R., Bearhop, S., Jackson, A.L., Moore, J.W., Parnell, A.C., Semmens,  
511 B.X., Ward, E.J., 2014. Best practices for use of stable isotope mixing models in food-  
512 web studies. *Can. J. Zool.* 835, 823–835.

513 Phillips, D.L., Newsome, S.D., Gregg, J.W., 2005. Combining sources in stable isotope  
514 mixing models: Alternative methods. *Oecologia* 144, 520–527. doi:10.1007/s00442-004-  
515 1816-8

516 Pougnet, F., Schäfer, J., Dutruch, L., Garnier, C., Tessier, E., Dang, D.H., Lancelot, L.,  
517 Mullot, J.-U., Lenoble, V., Blanc, G., 2014. Sources and historical record of tin and  
518 butyl-tin species in a Mediterranean bay (Toulon Bay, France). *Environ. Sci. Pollut. Res.*  
519 *Int.* 21, 6640–51. doi:10.1007/s11356-014-2576-6

520 Ramaswamy, V., Gaye, B., Shirodkar, P. V., Rao, P.S., Chivas, A.R., Wheeler, D., Thwin, S.,  
521 2008. Distribution and sources of organic carbon, nitrogen and their isotopic signatures  
522 in sediments from the Ayeyarwady (Irrawaddy) continental shelf, northern Andaman  
523 Sea. *Mar. Chem.* 111, 137–150. doi:10.1016/j.marchem.2008.04.006

- 524 Redfield, A.C., Ketchum, B.H., Richards, F.A., 1963. The Influence of Organisms on the  
525 Composition of Sea Water. *Sea*.
- 526 Ruttenberg, K.C., 2003. The Global phosphorus cycle, in: Turekian, K.K., Holland, H.D.  
527 (Eds.), *Treatise on Geochemistry*. Elsevier Ltd, pp. 585–643.
- 528 Savage, C., Leavitt, P.R., Elmgren, R., 2010. Effects of land use, urbanization, and climate  
529 variability on coastal eutrophication in the Baltic Sea. *Limnol. Oceanogr.* 55, 1033–  
530 1046. doi:10.4319/lo.2010.55.3.1033
- 531 Stephenson, R., Tan, F., Mann, K., 1986. Use of stable carbon isotope ratios to compare plant  
532 material and potential consumers in a seagrass bed and a kelp bed in Nova Scotia,  
533 Canada. *Mar. Ecol. Prog. Ser.* 30, 1–7. doi:10.3354/meps030001
- 534 Teranes, J.L., Bernasconi, S.M., 2000. The record of nitrate utilization and productivity  
535 limitation provided by d15N values in lake organic matter— A study of sediment trap  
536 and core sediments from Baldeggersee, Switzerland. *Limnol. Oceanogr.* 45, 801–813.  
537 doi:10.4319/lo.2000.45.4.0801
- 538 Tessier, E., Garnier, C., Mullet, J.-U., Lenoble, V., Arnaud, M., Raynaud, M., Mounier, S.,  
539 2011. Study of the spatial and historical distribution of sediment inorganic contamination  
540 in the Toulon bay (France). *Mar. Pollut. Bull.* 62, 2075–2086.  
541 doi:10.1016/j.marpolbul.2011.07.022
- 542 Ullman, W.J., Aller, R.C., 1980. Dissolved iodine flux from estuarine sediments and  
543 implications for the enrichment of iodine at the sediment water interface. *Geochim.*  
544 *Cosmochim. Acta* 44, 1177–1184. doi:10.1016/0016-7037(80)90071-X
- 545 UNEP, 2006. *Marine and coastal ecosystem and human well-being: A synthesis report based*  
546 *on the findings of the Millennium Ecosystem Assessment*.
- 547 Vaalgamaa, S., Sonninen, E., Korhola, A., Weckström, K., 2013. Identifying recent sources of  
548 organic matter enrichment and eutrophication trends at coastal sites using stable nitrogen  
549 and carbon isotope ratios in sediment cores. *J. Paleolimnol.* 50, 191–206.  
550 doi:10.1007/s10933-013-9713-y
- 551 Vitousek, P.M., Mooney, H. a, Lubchenco, J., Melillo, J.M., 1997. Human Domination of  
552 Earth's Ecosystems. *Science* (80-. ). 277, 494–499. doi:10.1126/science.277.5325.494

- 553 Wetz, M.S., Hales, B., Wheeler, P.A., 2008. Degradation of phytoplankton-derived organic  
554 matter: Implications for carbon and nitrogen biogeochemistry in coastal ecosystems.  
555 *Estuar. Coast. Shelf Sci.* 77, 422–432. doi:10.1016/j.ecss.2007.10.002
- 556 Xianhao, C., Weiping, X., Haisheng, Z., 1992. Remobilization and accumulation of iodine in  
557 marine sediments, Western Antarctic ocean. *Antarct. Res.* 3, 50–59.
- 558 Yokoyama, H., Abo, K., Ishihi, Y., 2006. Quantifying aquaculture-derived organic matter in  
559 the sediment in and around a coastal fish farm using stable carbon and nitrogen isotope  
560 ratios. *Aquaculture* 254, 411–425. doi:10.1016/j.aquaculture.2005.10.024
- 561

**Table 1**[Click here to download Table: Dang et al. Table 1.docx](#)**Table 1:** Concentration in OC, N, P, C/N ratio and C, N isotope composition in river particles, surface sediments and sediments core collected from Toulon Bay.

| Stations                  | {OC} in % (n)  | {N} in % (n)     | C/N (g g <sup>-1</sup> ) | δ <sup>13</sup> C (‰) | δ <sup>15</sup> N (‰) | {P} in g g <sup>-1</sup> (n) |                             |
|---------------------------|----------------|------------------|--------------------------|-----------------------|-----------------------|------------------------------|-----------------------------|
| Las river particles       | 0.9 ± 0.6 (5)  | 0.07 ± 0.04 (5)  | 14.5 ± 2                 | -28.5±0.8             | 5.0±0.9               | 410 ± 145 (5)                |                             |
| Eygoutier river particles | 3.0 ± 1.2 (5)  | 0.21 ± 0.09 (5)  | 13.7 ± 0.9               |                       |                       | 1240 ± 360 (5)               |                             |
| Surface sediments         | 3.9 ± 1.5 (59) | 0.11 ± 0.07 (9)  | 17.5 ± 3.5               | -24.5 to -19.8        | 0.5 to 4.5            | 530 ± 150 (59) <sup>a</sup>  |                             |
| MIS                       | 4.9 ± 1.3 (4)  | 0.25 ± 0.06 (4)  | 19.4 ± 3.9               | -25.5±1.1             | 4.0±0.8               | 850 <sup>b</sup>             | 1200± 350 (20) <sup>c</sup> |
| LAS1                      | 2.2 ± 0.6 (20) | 0.12 ± 0.03 (20) | 18.9 ± 1.8               | -28.6±0.6             | 1.4 to 2.8            | 2500 <sup>b</sup>            | 550± 90 (12) <sup>c</sup>   |
| LAS2                      | 2.5 ± 1.1 (25) | 0.21 ± 0.14 (25) | 14.5 ± 4.6               | -26.4±1.4             | 3.0±0.6               | 350 <sup>b</sup>             | 370± 60 (18) <sup>c</sup>   |
| 3B                        | 5.3 ± 1.2 (23) | 0.24 ± 0.04 (5)  | 18.6 ± 2                 | -21.5±0.6             | 4.8 to 8.9            | 1100 <sup>b</sup>            | 870± 90 (16) <sup>c</sup>   |
| 12                        | 4.9 ± 0.6 (29) | 0.24 ± 0.02 (5)  | 18.6 ± 1                 | -18.6±1.7             | 2.6 to 5.1            | 860 <sup>b</sup>             | 450± 40 (22) <sup>c</sup>   |
| 15                        | 6.8 ± 1.1 (28) | 0.24 ± 0.03 (8)  | 21.1 ± 2.3               | -16.8±1.7             | 1.7 to 4.9            | 760 <sup>b</sup>             | 320± 33 (21) <sup>c</sup>   |
| 23                        | 3.5 ± 0.6 (5)  | 0.12 ± 0.02 (5)  | 28.1 ± 3.2               | -17.9±0.7             | 1.8±0.2               | 500 <sup>b</sup>             | 300± 40 (13) <sup>c</sup>   |
| 52                        | 1.3 ± 1 (4)    | 0.08 ± 0.04 (4)  | 17.8 ± 4.4               | -22.6±0.6             | 0.2 to 1.9            | 540 <sup>b</sup>             | 360± 30 (14) <sup>c</sup>   |

<sup>a</sup> 0-5 cm; <sup>b</sup> 0-2cm; <sup>c</sup> -15 cm to sediment core bottom

## TABLES

**Table 1:** Concentration in OC, N, P, C/N ratio and C, N isotope composition in river particles, surface sediments and sediments core collected from Toulon Bay.

## FIGURES

**Figure 1:** Map of the study site showing main anthropogenic activities. Las and Eygoutier Rivers are discharging into little and large Bay, respectively. Two treated sewage submarine outlets discharge into large Bay. Cross symbols show the location of 54 surface sediments while circle symbols locate eight sediment cores. The numbers adjacent to cross symbols correspond to the surface sediment samples where C and N isotope compositions are analyzed.

**Figure 2:** Concentration in organic Carbon and total P in surface sediments (0-5 cm) of Toulon Bay.

**Figure 3:** Biplot of the relationship between C, N, and P in river particles and sediments of Toulon Bay. The OC/N relationship in Station-12 porewater is reported by Dang et al. (2014a).

**Figure 4:** Biplot of C and N isotope composition in rivers particles, surface and core sediments. The three area plots show data reported from the literature for freshwater phytoplankton (yellow), estuarine-marine phytoplankton (blue) and seagrasses/macroalgae (green). Refer to Figure S4 and Table S1 for more details. The black circles summarize the five potential sources used in the IsoSource program, while the grey circle positions the isotopic composition revealed in a wetland (Li et al., 2016).

**Figure 5:** Comparison of the modeled and observed C and N isotope composition by the multiple end-member mixing model. In the panel B, the symbol size is proportional to the contribution of Source4, the full line shows the regression passing through zero while the dashed line shows the regression line fitting the data.

**Figure 6:** Radar plots showing contributions of five sources at six sediment cores. Line-and-scatter plots show the average of the whole sediment core while line plots show the minimal and maximal values.

**Figure 7:** Total P vs.  $\delta^{15}\text{N}$ ; black circles show the relationship between total P and N isotope composition in bulk sediments. Colored symbols represent individual sediment cores while

comparing total P to anthropogenic N isotope composition with the relationship of  $P = 270 \times \delta^{15}N_{\text{anthr.}} + 415$ .

**Figure 8:** Comparison of total P to Iodine and Mg in surface sediments and sediment cores. Correlations are only observed for stations 15, 23 and 52.

**Figure 9:** Map of anthropogenic P loading in the Toulon Bay revealing non-point source (northern Little Bay) and point sources (aquaculture: station 15 and treated sewage: stations 39 and 42).

**Figure 10:** Estimated non-anthropogenic (diagenetic) P profiles at six stations (A) and the averaged profile (B). The non-anthropogenic P background is represented by the vertical red line and the variation range in total P of six sediment cores is shown by the grey zone in (B). Refer to Figure S2 for individual total P profiles.

Figure 1

[Click here to download high resolution image](#)

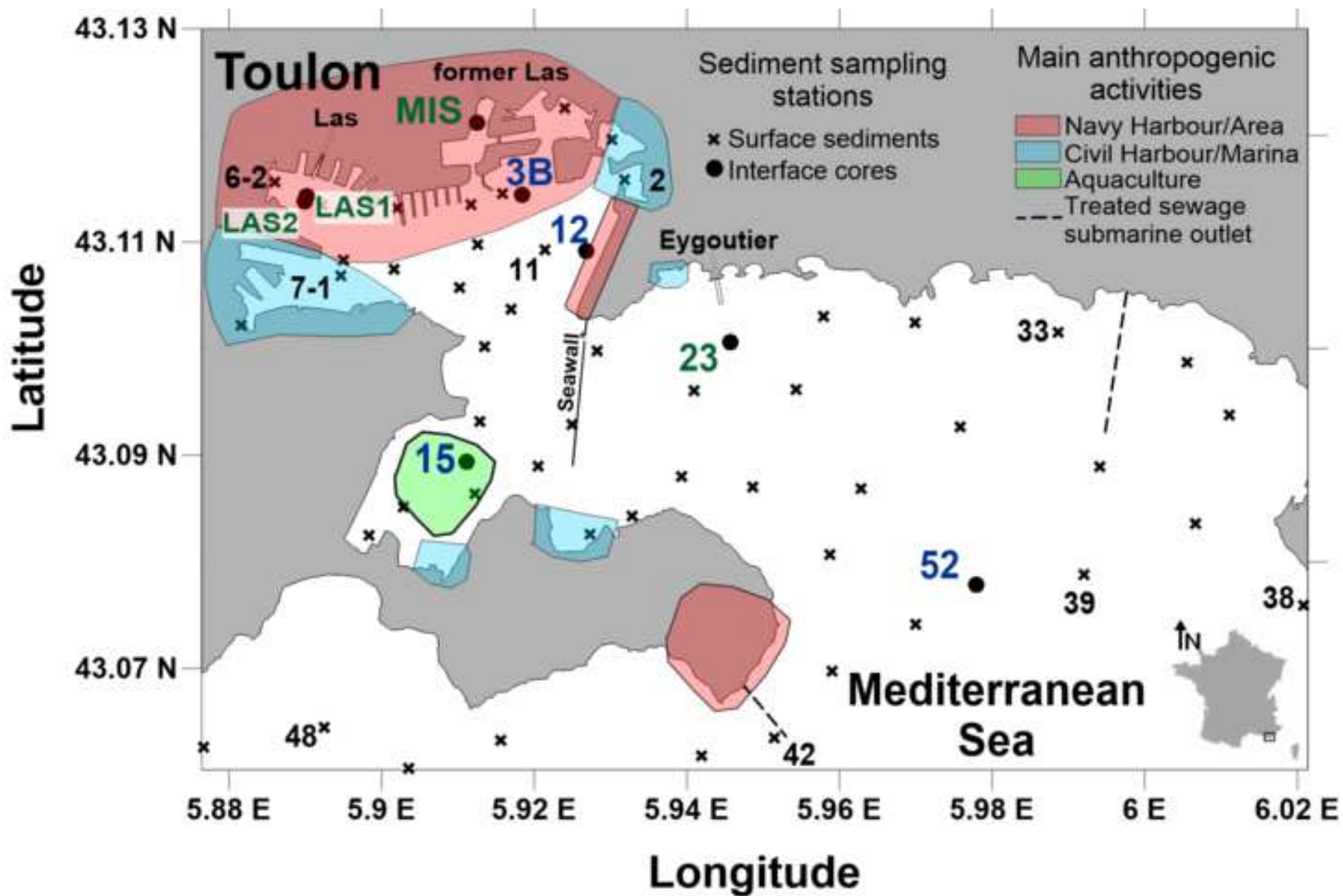


Figure 2  
[Click here to download high resolution image](#)

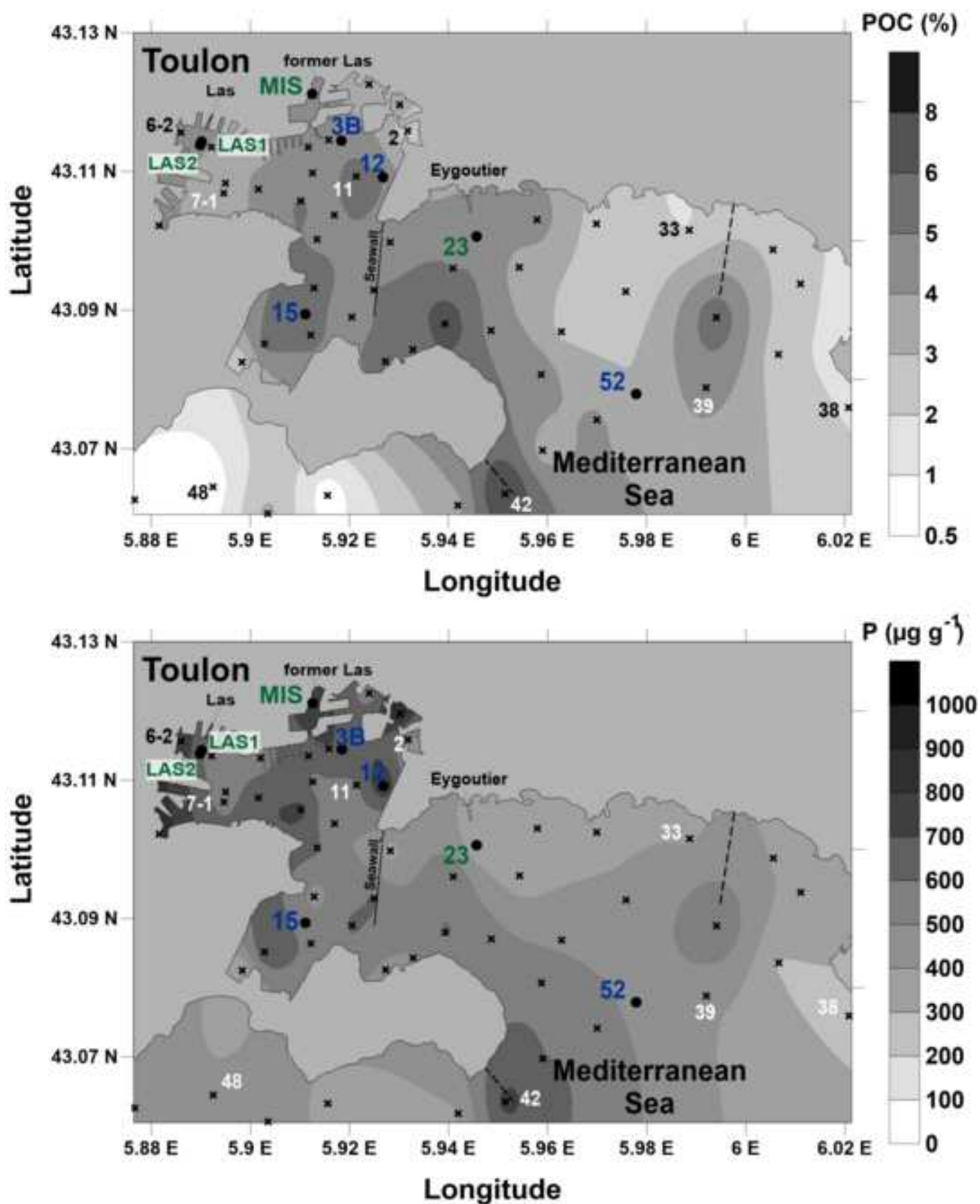


Figure 3

[Click here to download high resolution image](#)

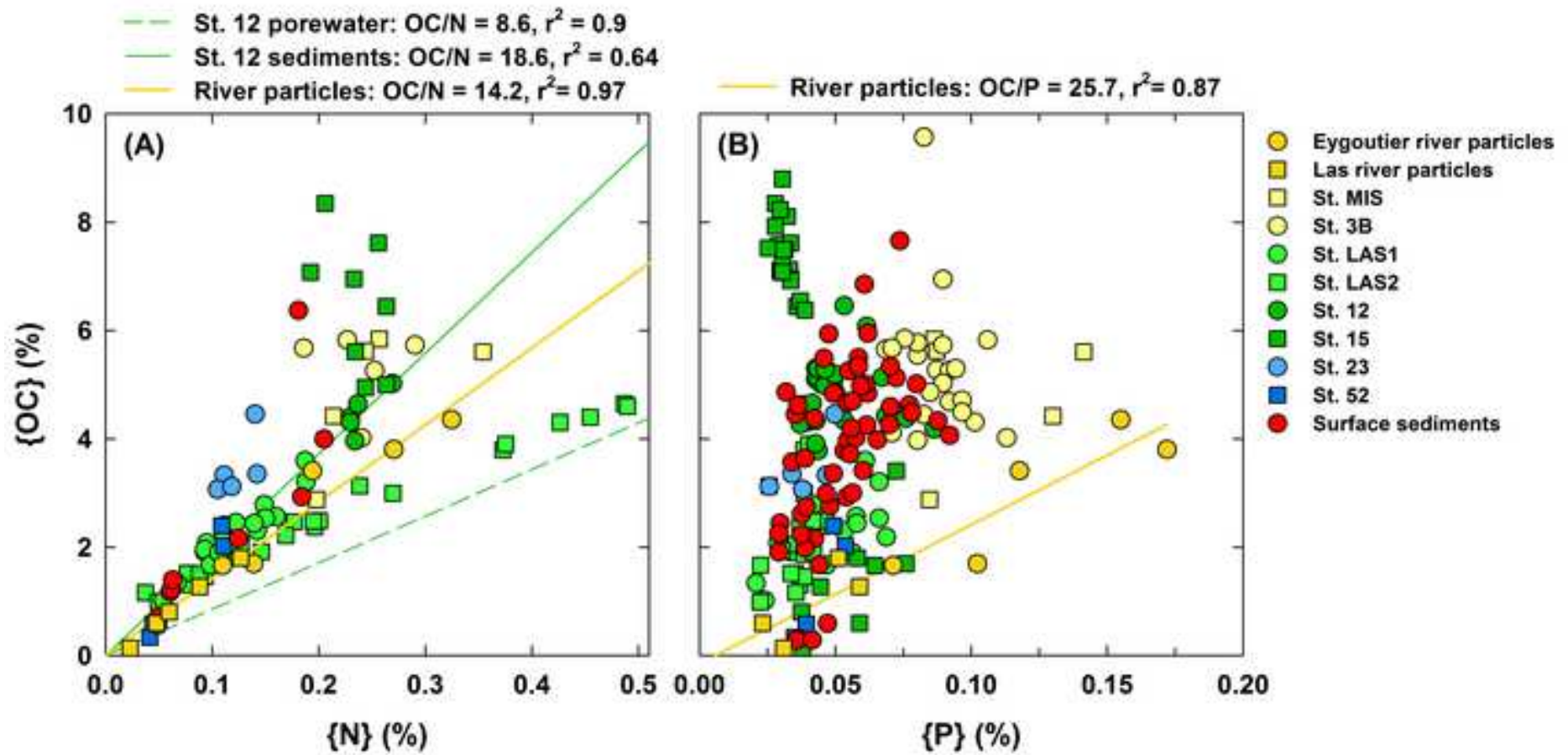


Figure 4

[Click here to download high resolution image](#)

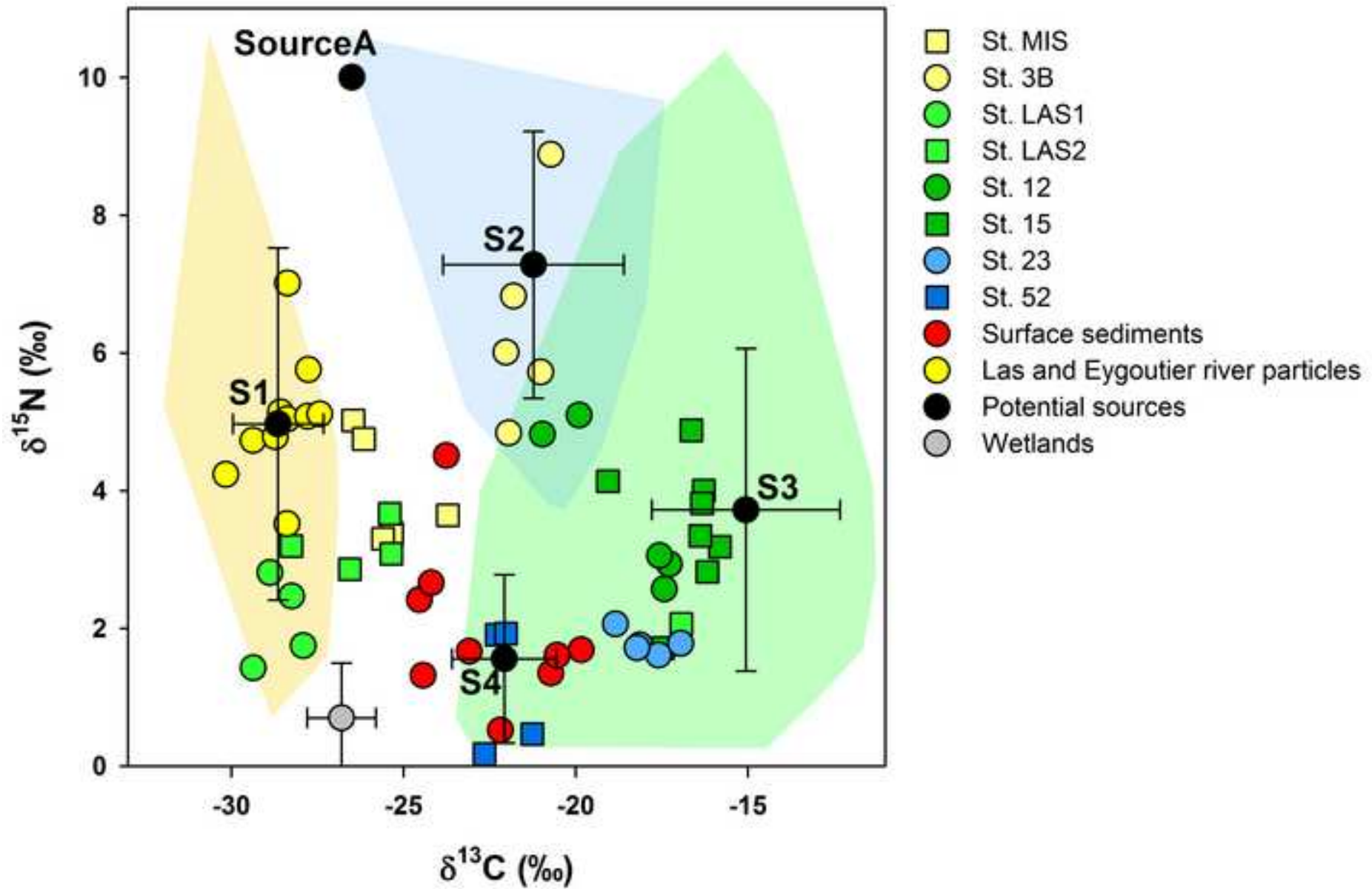


Figure 5

[Click here to download high resolution image](#)

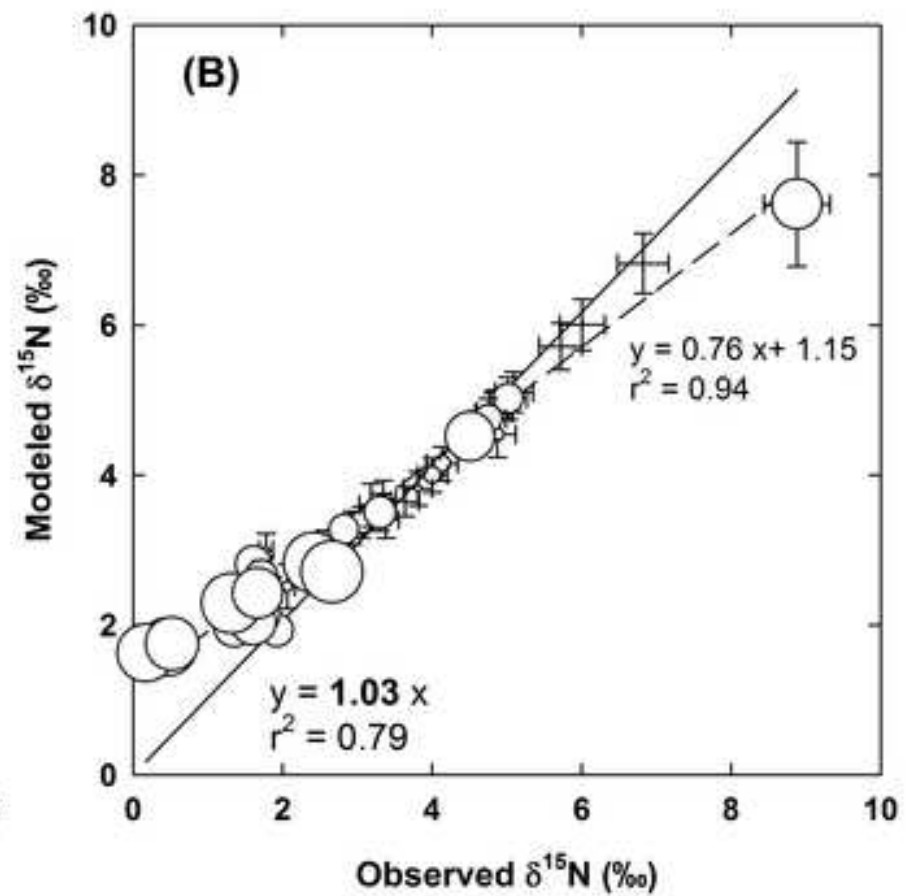
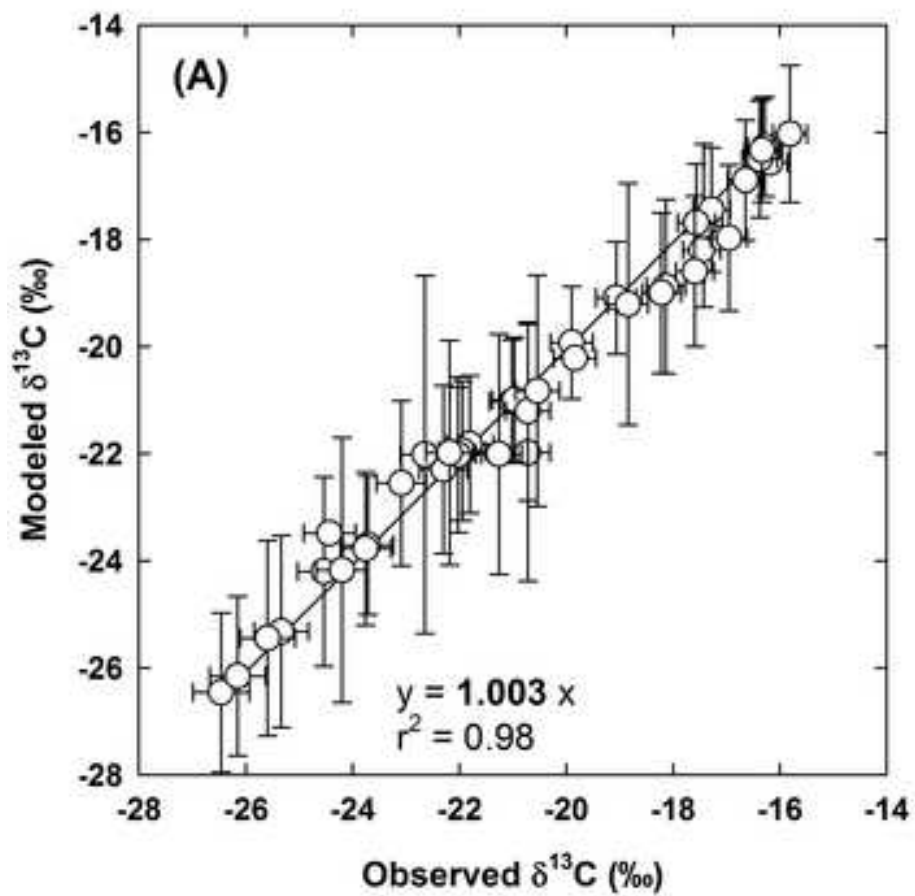


Figure 6

[Click here to download high resolution image](#)

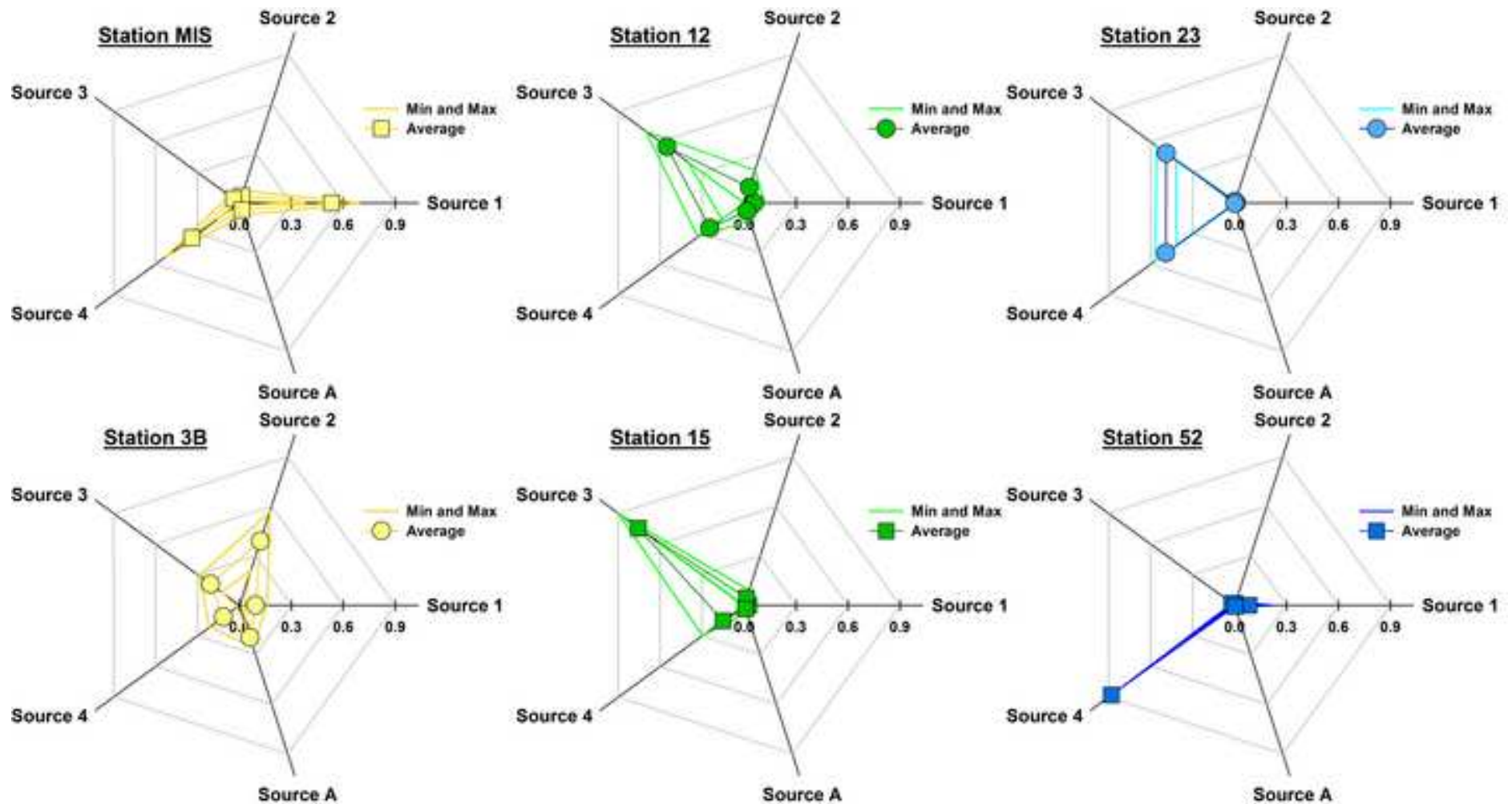


Figure 7

[Click here to download high resolution image](#)

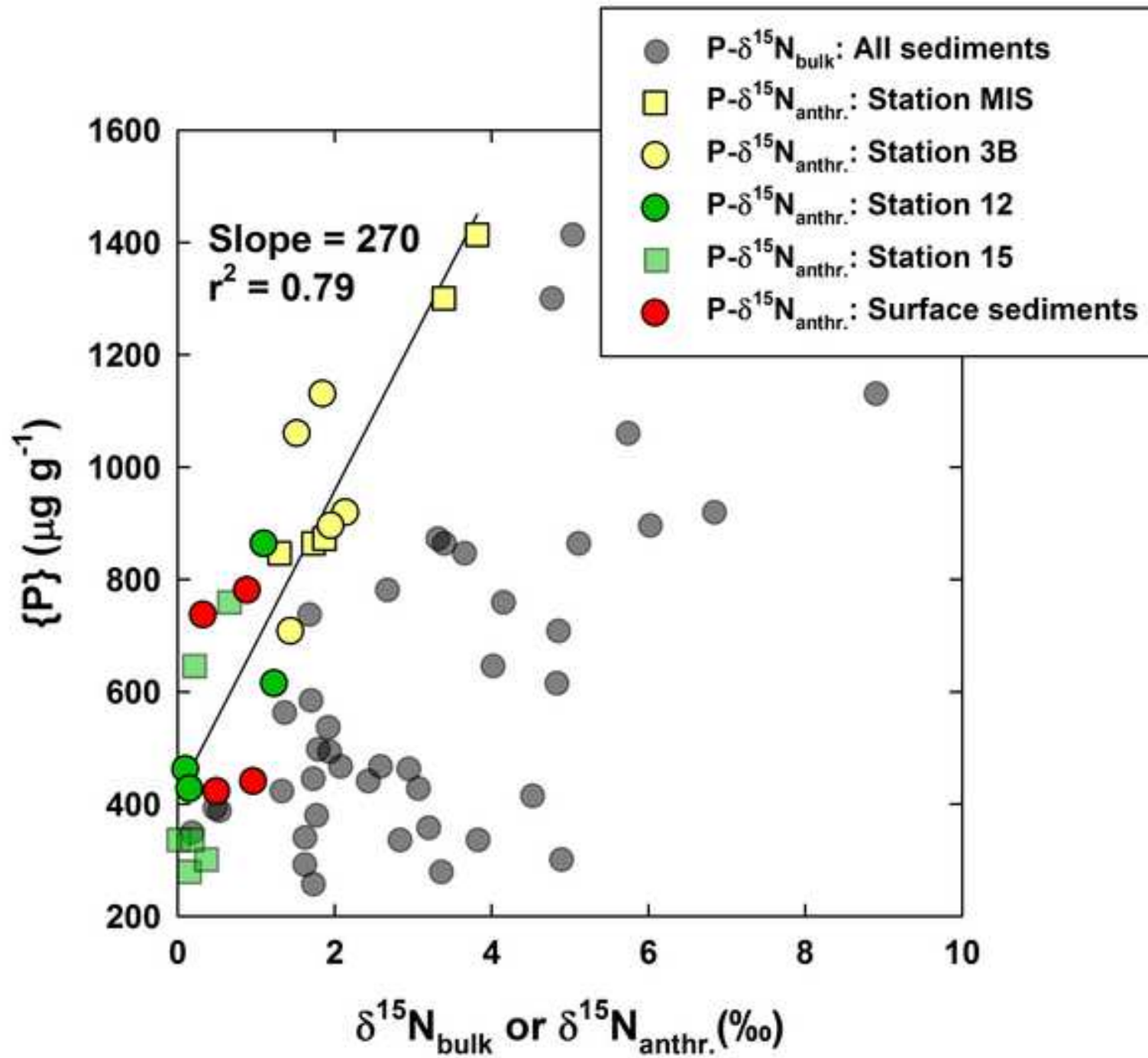


Figure 8

[Click here to download high resolution image](#)

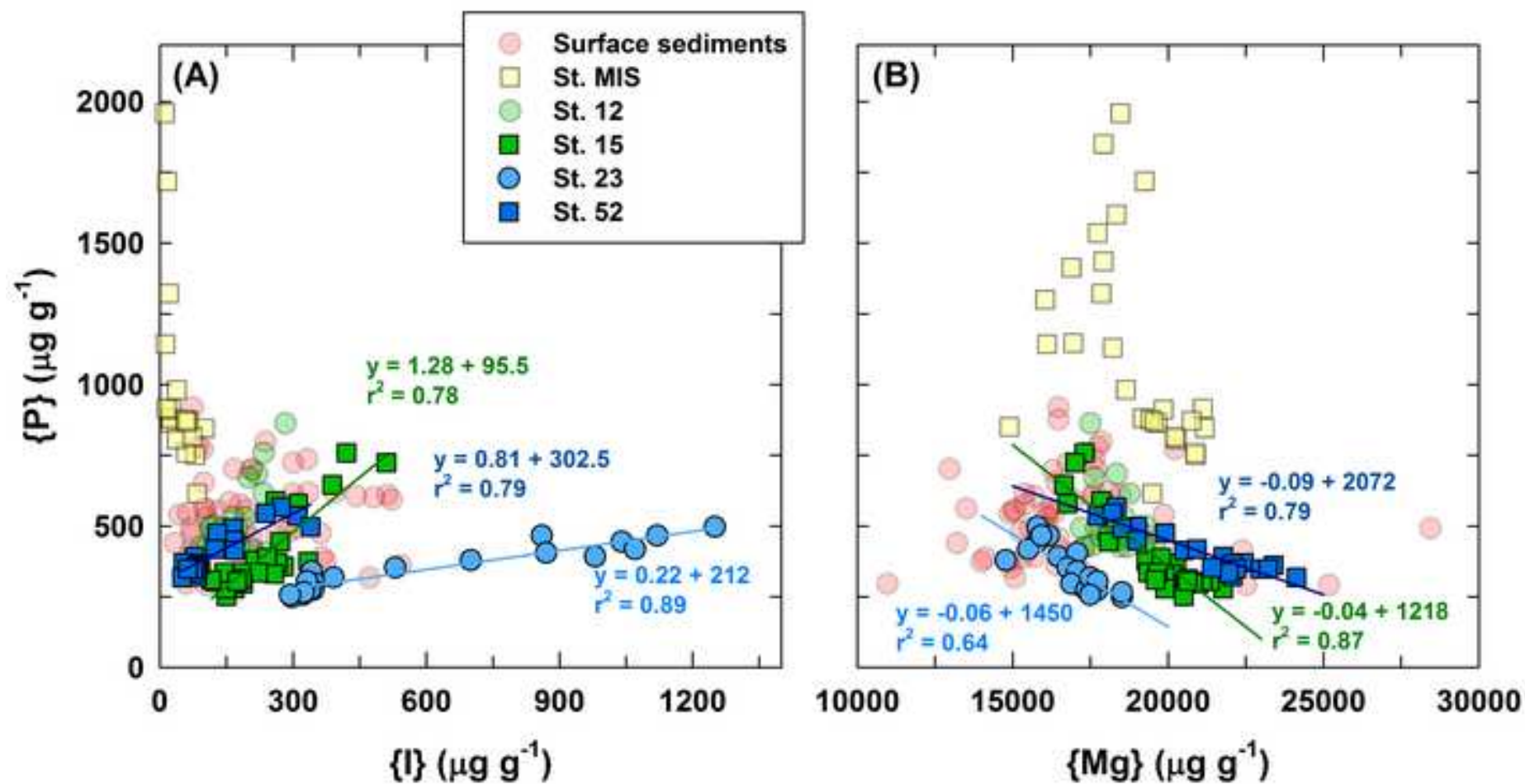


Figure 9

[Click here to download high resolution image](#)

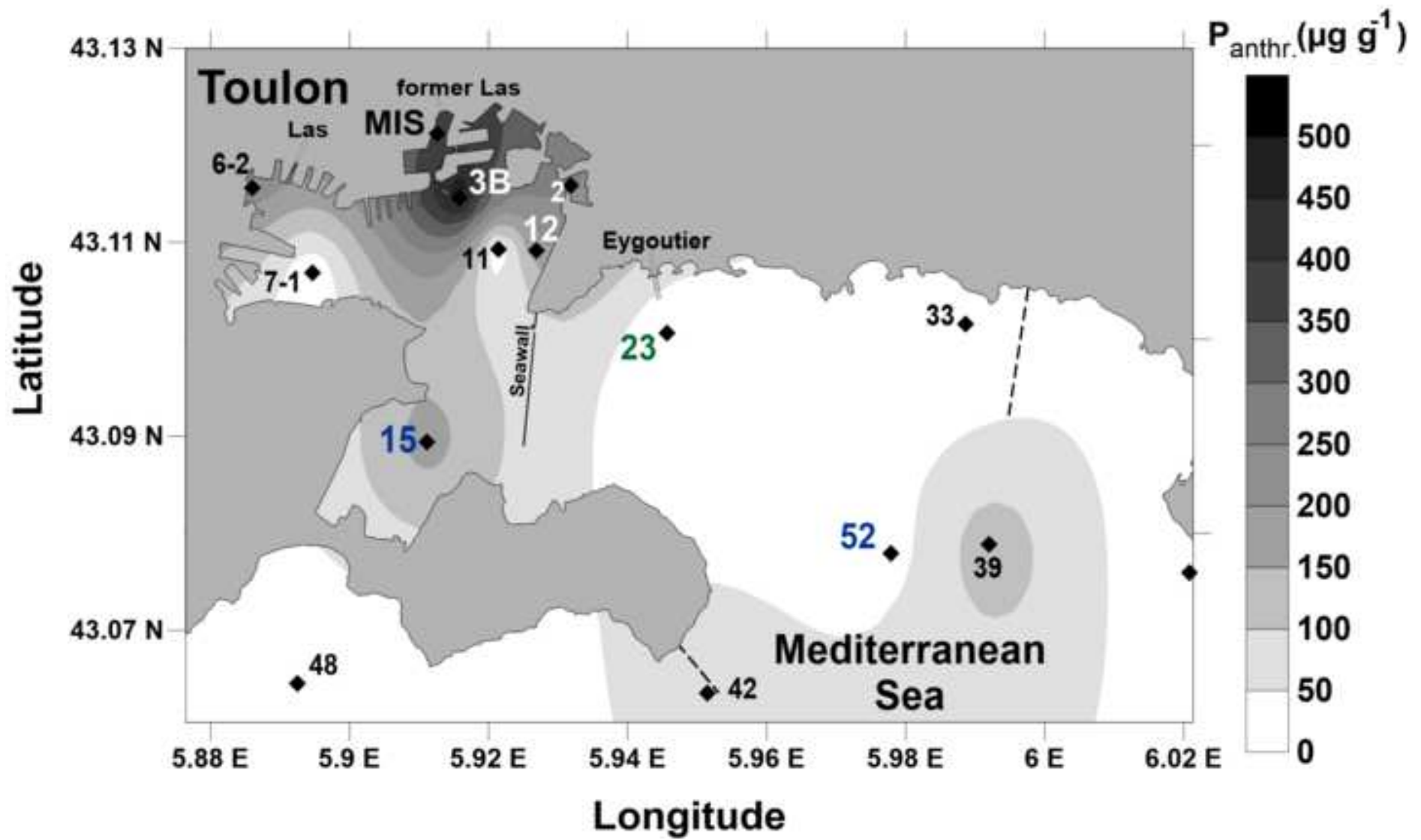
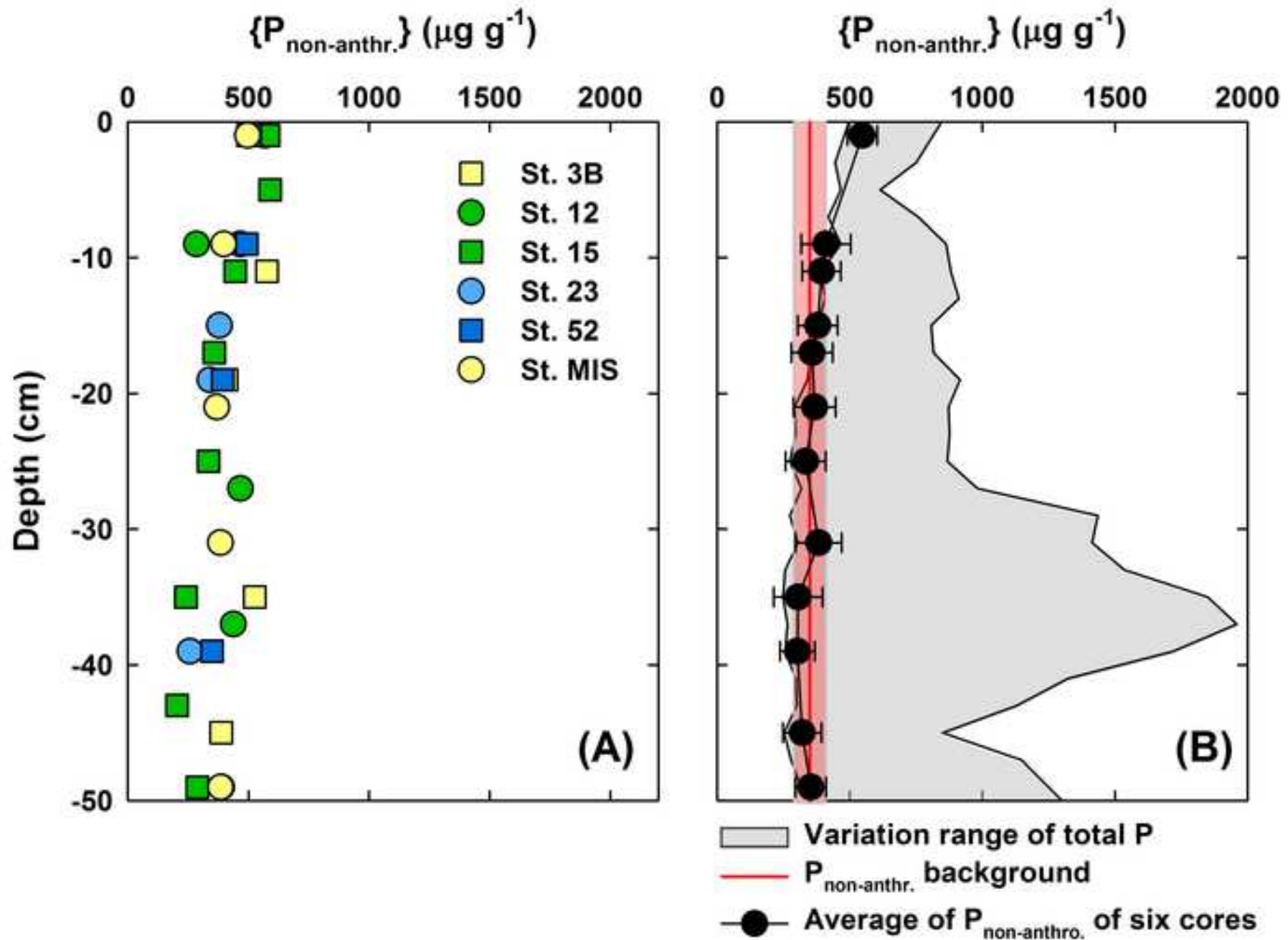


Figure 10

[Click here to download high resolution image](#)



**Electronic Supplementary Material (for online publication only)**

[Click here to download Electronic Supplementary Material \(for online publication only\): Dang et al. Supplementary information.p](#)